SENSITIVITY OF STRUCTURALLY LOADED SANDWICH PANELS TO LOCALIZED BALLISTIC PENETRATION

Jørgen A. Kepler*, Peter H. Bull**
, *: Department of Mechanical Engineering, Aalborg University, Denmark**

Keywords: *impact, penetration, sandwich, preload, damage*

Abstract

This paper describes the combination of structural loading (bending, shear) and simultaneous penetrating impact on sandwich panels with thin GFRP face-sheets, with emphasis on the damage morphologies and developments depending on the type and magnitude of structural loading. The test specimens were sandwich panels with length 250 mm and width 150 mm. The face-sheets consists of carbon fibre prepreg ([0°/90°], thickness $t_f \cong 0.5$ mm) bonded to the faces of a foam core (density 80 kg/m^3, thickness H = 10 mm). The impact velocity was approximately 420 m/s, using a spherical steel impactor, diameter 10mm, with a mass of approximately 4g. A high-speed camera was used for qualitative registration of panel response. It was demonstrated, that, at preload levels above a specific limit, the impact would cause catastrophic failure, i.e. complete or near-complete loss of structural integrity.

1 Introduction

In generalized terms, this paper treats the case of sudden, localized damage to an already prestressed structural component. The case may be seen as the temporal reversal of classical fracture mechanics (where a locally damaged component is subjected to a structural load). It will be experimentally demonstrated that the two situations share some characteristics, e.g. a threshold structural load level, below which the local damage does not propagate, and that the progression of damage follows the release of elastic energy. Specifically, the structural components treated in this paper were sandwich panels, consisting of thin, rigid face-sheets bonded to the opposing sides of a thick, low-density core plate. In an idealized representation of sandwich structures, external bending moment is balanced by opposing membrane forces in the face-sheets, while external transverse loads are balanced by transverse core shear. The specimens were subjected to symmetric or antisymmetric bending (corresponding to the aforementioned idealized situations) and local damage was caused by penetration of the specimen centre by a small-diameter steel impactor moving at high velocity.

The simultaneous combination of structural preload and localized impact is a potentially critical situation. Taken separately, the preload itself may be well within safety limits, and the puncture caused by a localized penetration without structural preload may be quite localized. In combination, however, the impact damage may initiate a damage process which eventually destroys the load carrying capacity of the structural component in question. Throughout this paper, such a process will be referred to as “catastrophic failure”.

Pressurized tubes, such as airplane fuselages and oil pipes, is a special case which has received some attention, see e.g. [1] by Rosenberg *et al*. In a recent study by Lu et al. [2], the “ballistic limit” of low-velocity impact on water-filled, pressurized metal pipes was studied.

Similar combined loading on sandwich structures has apparently been largely neglected, despite the fact that sandwich structures, due to the high stiffness/weight-ratio, are frequently used in transportation applications and so are susceptible to impact loads in general. In [3], Abrate commented on the general scarcity of papers on ballistic penetration of sandwich panels. In a recent paper, [4], Malekzadeh *et al*. described a model for predicting the contact force and panel response when subjecting an in-plane prestressed sandwich panel to low velocity, nonpenetrating impact. It was, among other things, demonstrated that the peak contact force would increase and the deflection decrease with increasing tensile preload. However, the matters of overall structural response and possible catastrophic failure following penetrating impact

were not addressed. A similar case for composite laminates was studied by Mitrevski et al. [5], who subjected test specimens to in-plane biaxial load and simultaneous transverse impact. A stiffening effect due to biaxial tension preload was observed, similarly to the results mentioned in [4], while damage sizes and absorbed energy was largely unaffected. Hertzberg and Weller studied a special case, impact on buckled composite panels, where an impact occurred on the convex or concave panel side, see [6]. Although the panels considered were not of sandwich type, the considerations of catastrophic damage and impact on convex or concave composite panels have a direct relation to the issues considered in the present paper.

2 Procedures and test specimens

Two structural preload cases were considered, symmetric and antisymmetric. While subjected to an appropriate preload level, the specimens were penetrated by a small, spherical steel impactor. The situations are outlined in figure 1.

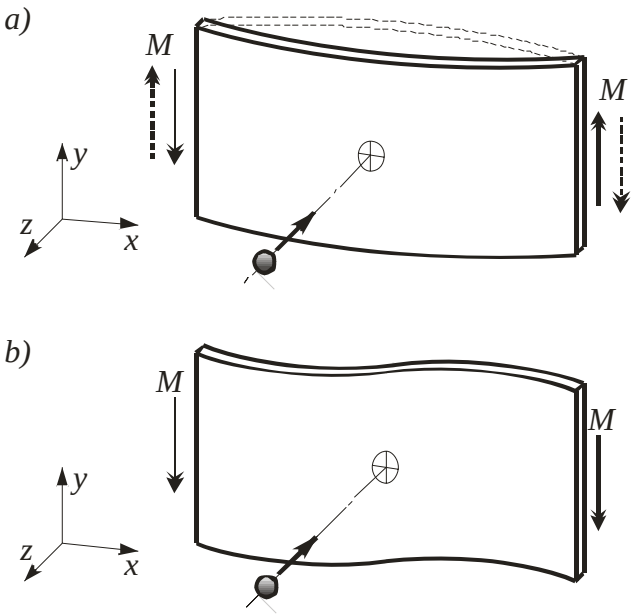

Fig. 1. Preload and impact scenarios. The panels were simply sypported along the vertical (y-direction) edges and subjected to bending moment M along the supported edges.
a): Symmetric bending – only the fully outlined case, with tension in the front face sheet, was considered.
b): Antisymmetric bending, with constant core shear stress along the specimen length.

A number of formally identical test specimens with a free specimen length of 250 mm and width 150 mm were manufactured. The material composition was:

Lamina: UD prepreg, T700 carbon fibre with SE84LV epoxy resin, fibre mass 300 g/m^2, fibre volume fraction 60%, total mass 476 g/m^2, effective thickness 0.25 mm per lamina.

Core: Polymethacrylimide (PMI) -foam, Rohacell 71 IG, thickness 10 mm

Core end inserts: Mild steel, thickness 10 mm

Sandwich layup [0°/90°/(core)/90°/0°], total effective face-sheet thickness t_f = 0.50 mm (per face-sheet, verified by microscopy).

The steel core inserts were used as core material at the preload application ends. The test specimen geometry is shown in figure 2. For the symmetric bending tests, the compressed face-sheets were reinforced in the transition zone between steel core inserts and foam core.

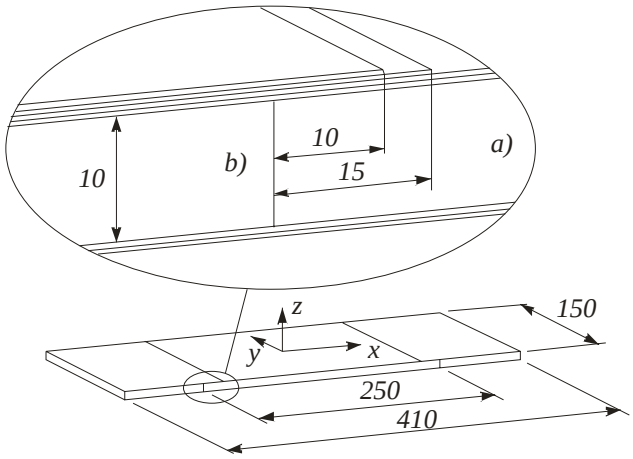

Fig. 2. Specimen geometry. All dimensions in mm. The specimen is symmetric about the yz-plane. The magnified view shows the local reinforcement of the compressed face sheet ([0°/90°/0°/90°] dropping to [90°/0°/90°] dropping to [0°/90°]) in the transition zone between steel core (b) and foam core (a).

The specimens were manufactured in three stages:

1) Steel core inserts and foam core were bonded, using a 2-component epoxy adhesive, and left to cure for several days.
2) [0°/90°] face-sheet plies were applied and cured in a vacuum bag at elevated

temperature, as outlined in the appropriate data-sheet.

3) Reinforcement plies added on compressive side face-sheet, cured as primary plies.

The structural preloads were applied to the steel-insert end zones of the specimens . The free-body diagrams in figures 3 and 4 indicate the resulting moment and shear distributions.

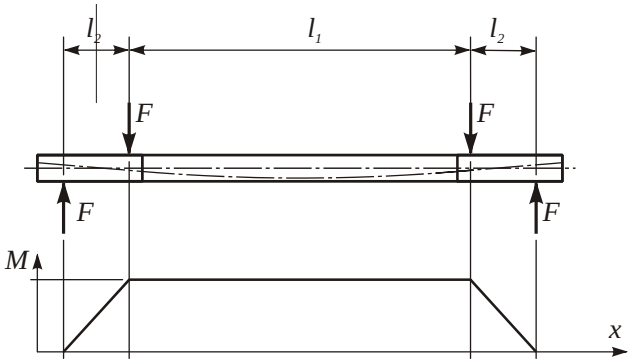

Fig. 3. Free-body diagram and moment distribution, symmetric bending. The dashed line indicates specimen deformation. Constant moment M along the free specimen length.

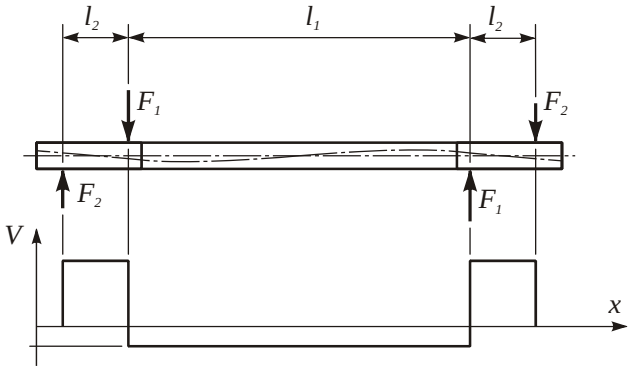

Fig. 4. Free-body diagram and shear distribution, antisymmetric bending. The dashed line indicates specimen deformation. Constant shear V along the free specimen length.

3 Static tests

For determining the maximum feasible preload level, a number of specimens were tested to failure in a quasi-static test setup (without impact).

On the specimens subjected to symmetric bending, strain gauges were bonded to the face sheets to provide a measurement of the preload-induced strain in the x-direction. 3 specimens were tested, giving an average ultimate preload ε_{ult} = 4400 μstrain. All three specimens failed by compressive face-sheet failure in the transition zone between steel and foam core, indicating a moderate amount of local face-sheet bending.

Two specimens were subjected to antisymmetric bending and failed at an average equivalent ultimate core shear stress of τ_{ult} = 1.18 MPa. The failure mode was core fracture at an angle of 45° relative to the specimen midplane. The core material manufacturer indicates an ultimate core shear stress of 1.30 MPa.

4 Combined preload and impact tests, setups

The tests with simultaneous structural preload and impact were conducted using a combination of gas gun, preload frame and high-speed camera. The impactor, a 10mm steel sphere, mass 4.1 g, would in all tests impact the specimen at a velocity of 415-420 m/s.

The test setups for the two different types of preload (symmetric – constant bending moment, and antisymmetric – constant shear force) are shown in figures 5 and 6.

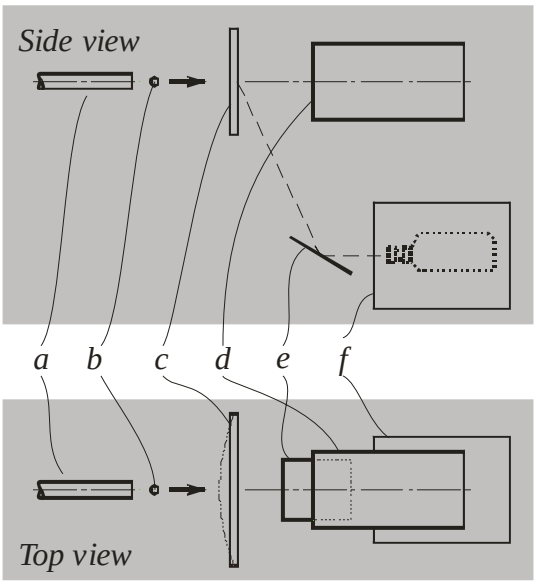

Fig. 5. Schematic of test setup for symmetric preload. The parts are:
a: Gas gun barrel
b: Impactor (10mm steel bullet)
c: Test specimen
d: Bullet catcher
e: Mirror
f: High-speed camera in steel box

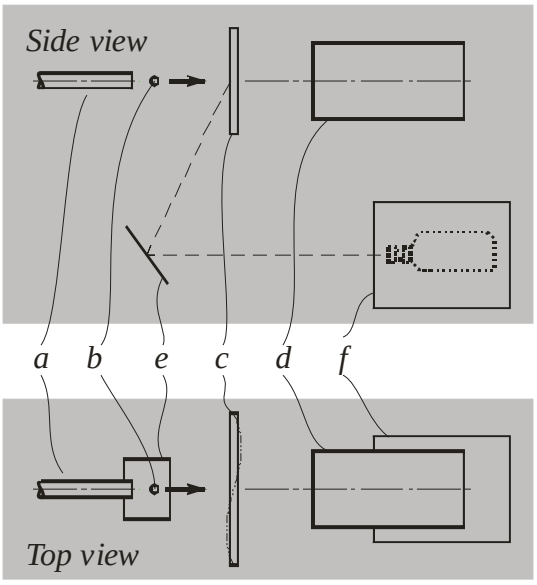

Fig. 6. Schematic of test setup for antisymmetric preload. The parts a-f are identical to those shown in figure 5.

Initial tests on impact with symmetrical bending had revealed that catastrophic damage was initiated by impact-induced debonding of the back face-sheet. Consequently, the mirror was placed to permit a back side view in the symmetric preload cases. In the antisymmetric cases, the mirror was placed to permit a front side view.

5 Results, symmetric bending preload + impact

With a ultimate static preload corresponding to a face sheet strain ε_{ult} = 4400 μstrain (as indicated in section 3), it was decided to set a maximum preload level corresponding to 0.6 ε_{ult}. Furthermore, with only 5 test specimens available for this test scenario, it was decided to start with the maximum preload level test and decrease the preload, until no catastrophic damage occurred. The results are outlined in table 1.

Table 1: Result outline, symmetric bending preload + impact.

Test number	Preload strain	Catastrophic damage	Penetration
c-s-020	0.2 ε_{ult}		+
c-s-040	0.4 ε_{ult}	+	+
c-s-045	0.45 ε_{ult}	+	+
c-s-050	0.5 ε_{ult}	+	+
c-s-060	0.6 ε_{ult}	+	+

6 Results, antisymmetric bending preload + impact

The ultimate static preload corresponded to an equivalent tranverse core shear stress τ_{ult} = 1.18 MPa (as indicated in section 3). Again, 5 specimens were available, and the test series was initiated at preload level 0.6 τ_{ult}. The results are outlined in table 2.

Table 2: Result outline, antisymmetric bending preload + impact.

Test number	Preload stress	Catastrophic damage	Penetration
c-a-020	0.2 τ_{ult}		+
c-a-040	0.3 τ_{ult}		+
c-a-045	0.4 τ_{ult}	+	+
c-a-050	0.5 τ_{ult}	+	+
c-a-060	0.6 τ_{ult}	+	+

7 High-speed camera recordings

The impact tests were recorded using an Olympus i-Speed 2 camera. The recording speed was 8000 frames/s and the frame size was 256x192 pixels. For the symmetric bending tests, the camera

viewed the back side of the specimen, while for the antisymmetric tests, the front side was viewed. Two 650 W photo-lamps were used to obtain sufficient light for the high-speed recordings. For better recording contrast, the specimens were painted matt white, and a 20 mm square grid was drawn using a black permanent ink marker. Furthermore, the predominantly white surface reduces heating problems caused by the photo-lamps. Even so, the photo lamps should not be turned on more than a few seconds before shooting – a test specimen in an early test series failed due to thermal stresses. Figures 7 and 8 shows the first 8 frames (0.875 ms) of test c-s-045 and c-a-060, respectively.

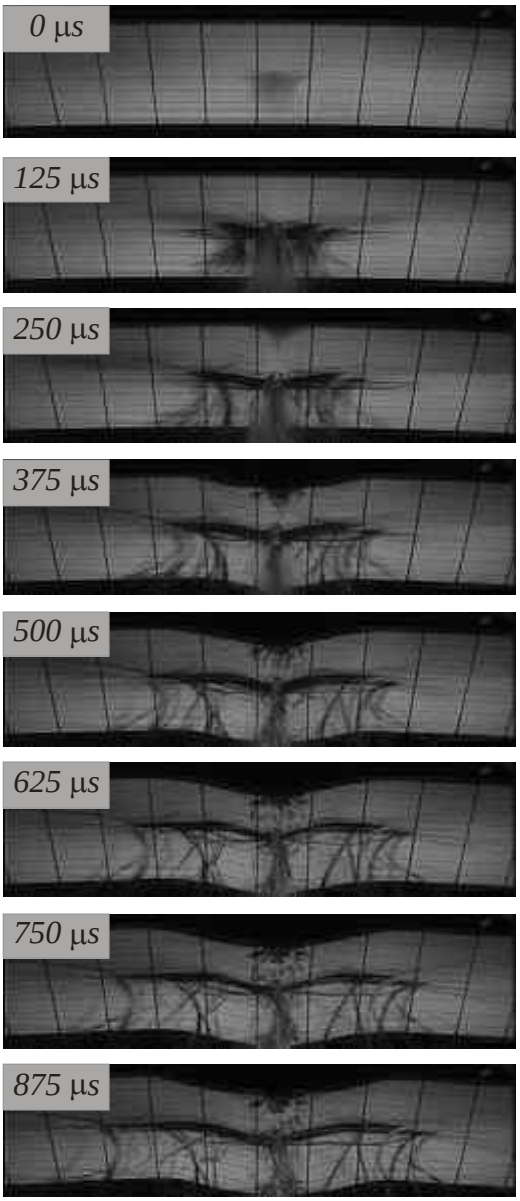

Fig. 7. High-speed camera recordings showing back side view of specimen c-s-045, from 0 to 0.875 ms.

In figure 7, the initial frame (0 μs) shows a trace of the impactor exiting the test specimen.

At 125 μs, a plume of ejecta is seen – the intensity of the plume is reduced in subsequent frames. Also, strips of 0° fibres are peeling off to both sides of the impact point – this becomes more visible in subsequent frames. Near the impact point, a barely visible bulge indicates debonding between core and back face-sheet.

At 250 μs, the debonding bulge appears to have just reached the edge of the specimen, thus extending across the specimen width.

From 375 μs onwards, the length of the debonding bulge grows visibly, and the test specimen eventually retains negligible bending stiffness.

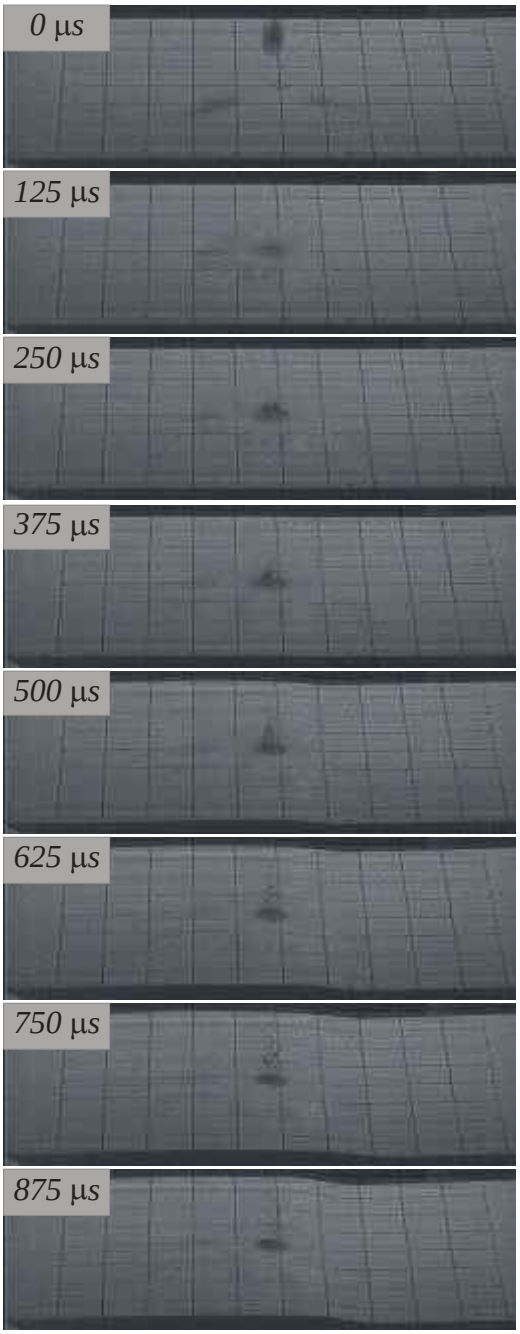

Fig. 8. High-speed camera recordings showing back side view of specimen c-a-060, from 0 to 0.875 ms.

In figure 8, the initial frame (0 μs) shows the impactor just before hitting the test specimen. The dark spots on the specimen surface are shadow outlines of the impactor, cast by the photolamps.

At 250 μs, a rearward plume of ejecta is beginning to form – this is believed to be caused by the formation and subsequent elastic springback of a debonding bulge on the back side of the specimen.

From the images in figure 8, it appears that shear failure occurs simultaneously across the width of the panel, initiating at about 500 μs. Closer scrutiny of the recordings reveal initiation of panel failure at about 375 μs, starting in the central part of the specimen

From 500 ms onwards, the specimen failure proceeds, as the face-sheet – core interface fails, reducing the shear carrying capacity of the panel.

8 Interpretation of failure sequences

Based on the camera recordings and subsequent post-impact analysis of the panels, the (speculative) failure progression is outlined in figures 9 and 11.

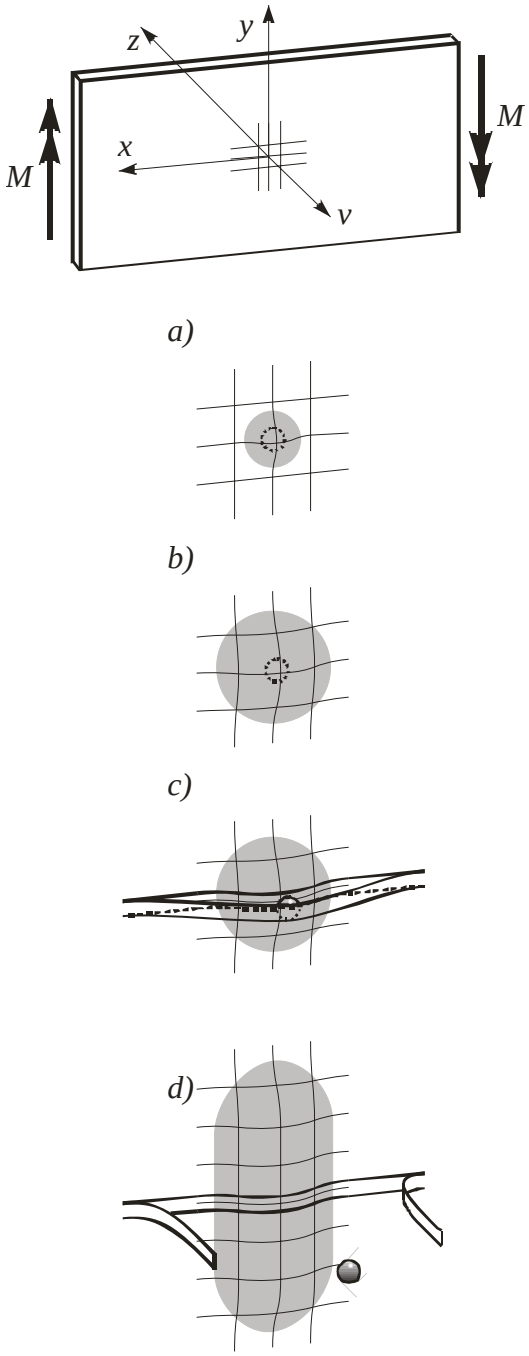

Fig. 9. Failure progression, symmetric bending. Top: Specimen, seen from the back side. v indicates the impactor velocity. a) to d): magnified view of the central area at different stages of penetration.

The impactor is represented as a sphere with dashed outline (when hidden) or full outline (when exposed).

a: onset of debonding between back face-sheet and core.

b: maximum debonding size, beginning face-sheet failure

c: tearoff of central strip of outer (0°) ply

d: debonding front progressing in y-direction

When the debonding front has reached the edges, the structural capacity is governed by the bending stiffness of the face-sheets (or, more precisely, the post-buckling behavior of the compressive side face-sheet), as seen in figure 10.

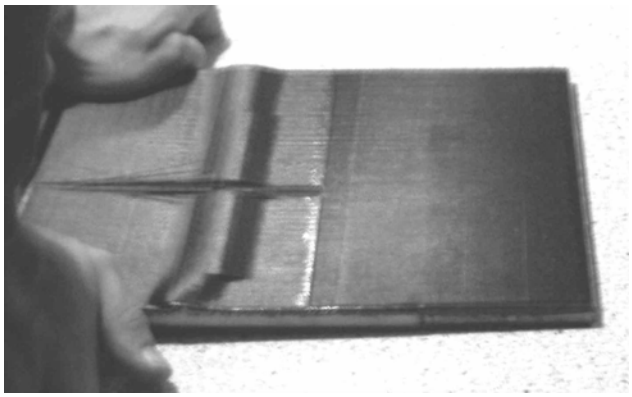

Fig. 10. Buckling of debonded compressive side face-sheet.

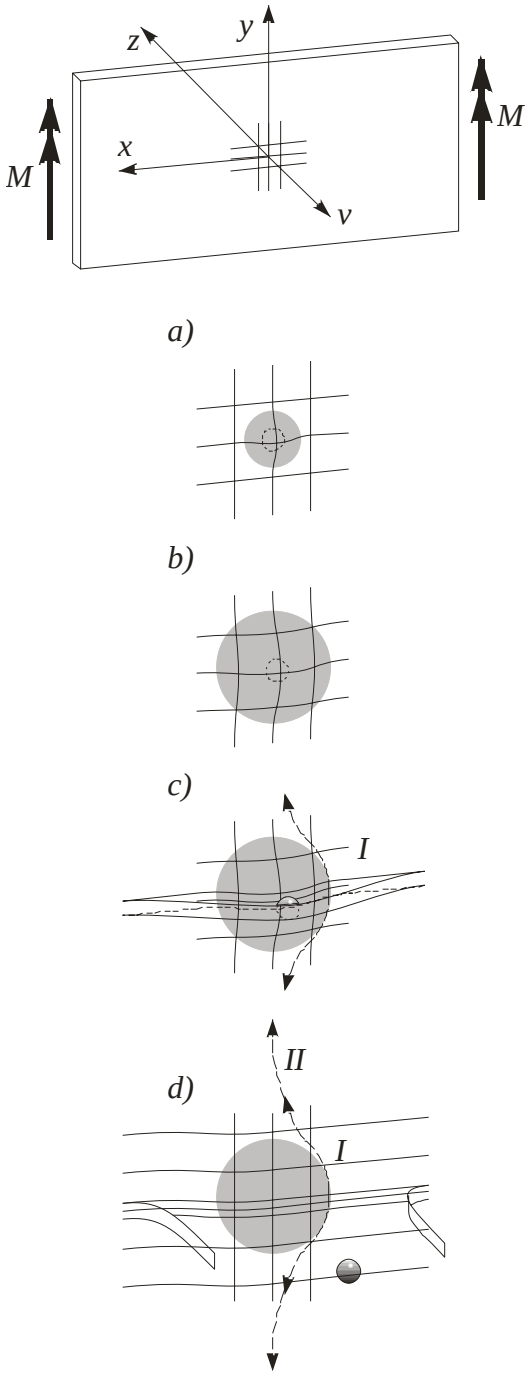

Fig. 11. Failure progression, antisymmetric bending. Top: Specimen, seen from the back side. v indicates the impactor velocity. a) to d): magnified view of the central area at different stages of penetration.
The impactor is represented as a sphere with dashed outline (when hidden) or full outline (when exposed).
a: onset of debonding between back face-sheet and core.
b: maximum debonding size, beginning face-sheet failure
c: tearoff of central strip of outer (0°) ply, mode I transverse core fracture propagating in ± y-direction
d: Failure of central strip of outer ply, core crack kinking progressively towards shear mode failure (mode II).

Eventually, the core fracture extends across the width of the specimen, whereupon the face-sheets separate from the core. The residual stiffness is, as in the case of symmetric bending, governed by the bending stiffness of the face-sheets. This is shown in figure 12.

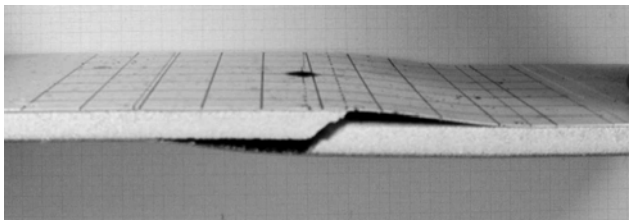

Fig. 12. Fully developed sandwich panel shear failure with extensive debonding between core and face-sheets.

9 Discussion and conclusion

The experiments described in the present paper demonstrated the possibility of catastrophic failure in a structurally preloaded sandwich panel when subjected to rapid, localized penetration. Although based on a severely limited number of experiments, the data nevertheless indicate a threshold preload level, above which the impact-induced damages will propagate. For the two preload cases treated in the present study, the threshold levels were between 20 and 40% of the corresponding ultimate static load.

In both cases, the onset of catastrophic failure was (speculatively) attributed to impact-induced debonding between the core and the back face-sheet. Post-impact analysis of specimens loaded below the threshold revealed a circular debonding of approximately 35 mm in diameter. Since this corresponds to an equivalent reduction of the sandwich panel width, it would be instructive to repeat the experiment with panels of larger width.

Constructive countermeasures against catastrophic failure should, in both load-cases, focus on increasing the strength/toughness of the interface between face-sheets and core. Post-impact analysis of the test-specimens revealed a poor interface strength, probably due to the omission of an additional adhesive film (the pre-pregs were applied

directly to the foam core surface). More radical measures include peel-stoppers and through-the-thickness stitching.

10 Acknowledgments

The work presented was supported by:

- The Innovation Consortium "Integrated Design and Processing of Lightweight Composite and Sandwich Structures" (abbreviated "Komposand"), funded by the Danish Ministry of Science, Technology and Innovation and the industrial partners Composhield A/S, DIAB ApS (DIAB Group), Fiberline Composites A/S, LM Glasfiber A/S and Vestas Wind Systems A/S.
- US Navy, Office of Naval Research (ONR), Grant/Award No. N000140710227: "Influence of Local Effects in Sandwich Structures under General Loading Conditions & Ballistic Impact on Advanced Composite and Sandwich Structures". The ONR program manager was Dr. Yapa Rajapakse.

The support received is gratefully acknowledged

References

[1] Rosenberg, Z., Mironi, J., Cohen, A. and Levy, P., On the Catastrophic Failure of High-pressure Vessels by Projectile Impact. *International Journal of Impact Engineering*, Vol. 15 p. 827-831, 1994.

[2] Lu, G. Y., Zhang, S. Y., Lei, J. P. and Yang, J. L. Dynamic Responses and Damages of Water-filled Pre-pressurized Metal Tube Impacted by Mass. *International Journal of Impact Engineeing*, Vol. 34 p. 1594-1601, 2006.

[3] Abrate, S. *Impact on Composite Structures*. 1st edition, Cambridge University Press, 1998.

[4] Malekzadeh, K., Khalili, M. R. and Mittal, R. K., Response of In-plane Linearly Prestressed Composite Sandwich Panels with Transversely Flexible Core to Low-velocity Impact. *Journal of Sandwich Structures and Materials*, Vol.8 p. 157-181, 2006.

[5] Mitrevski, T., Marshall, I. H., Thomson, R. S. and Jones, R., Low Velocity Impacts on Preloaded GFRP Specimens with Various Impactor Shapes. *Composite Structures*, Vol. 76 p. 209-217, 2006.

[6] Herszberg, I. and Weller, T., Impact Damage Resistance of Buckled Carbon/Epoxy Panels. Composite Structures, Vol. 73 p. 130-137, 2006